JACS
JOURNAL OF THE AMERICAN CHEMICAL SOCIETY
Article
pubs.acs.org/JACS

New Photolabile BAPTA-Based Ca^{2+} Cages with Improved Photorelease

Jiaxi Cui,[†] Radu A. Gropeanu,[†] David R. Stevens,[‡] Jens Rettig,[‡] and Aránzazu del Campo*[,†]

[†]Max-Planck-Institut für Polymerforschung, Ackermannweg 10, 55128 Mainz, Germany
[‡]Physiologisches Institut, Universität des Saarlandes, 66421 Homburg, Germany

Supporting Information

ABSTRACT: The efficient synthesis, physicochemical and photolytical properties of a photoactivable BAPTA-based Ca^{2+} cage containing two photosensitive o-nitrobenzhydryl groups attached to the aromatic core are described. Ca^{2+} release in living cells was evaluated. The double substitution with the chromophores caused a significant improvement of the Ca^{2+} release properties of nitr-T versus singly substituted reported nitr-x derivatives without compromising Ca^{2+}/Mg^{2+} selectivity or pH insensitivity. Our results demonstrate a general strategy to improve light-triggered Ca^{2+} release which may result in more efficient, selective, and pH-insensitive photolabile Ca^{2+} chelators.

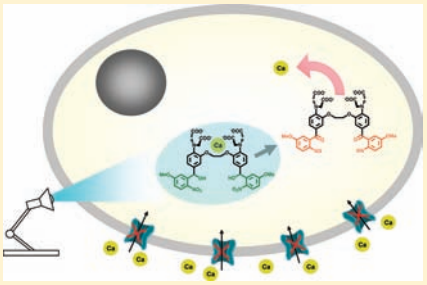

INTRODUCTION

Ionic calcium (Ca^{2+}) is one of the most important second messengers in cells.[1] Localized fluctuations of intracellular free Ca^{2+} concentration can regulate a variety of cellular functions, e.g., nerve impulses, muscle contraction, secretion, ion channels in the plasma membrane, or nonmuscle motility. To obtain sudden jumps of intracellular calcium ions, different photolabile caged Ca^{2+} molecules have been developed during the past 25 years.[1−3] Light irradiation of calcium cages releases free Ca^{2+} in solution and triggers the biological response. Caged Ca^{2+} compounds are now a well established working tool for studies in cellular physiology and neurobiology.[1]

When designing photolabile Ca^{2+} chelators, different requirements need to be considered: (1) chemical yield of Ca^{2+} release; (2) cation binding selectivity; (3) effectiveness of light absorption (the extinction coefficient and 2-photon cross section) and photochemical yield; (4) rate of Ca^{2+} release and (5) pH sensitivity of cation binding. So far, available photolabile Ca^{2+} chelators are not able to satisfy all of these requirements.[1] EDTA-based chelators like DM-nitrophen delivers Ca^{2+} very efficiently upon photolysis, but has a low Ca^{2+}/Mg^{2+} selectivity (500-fold) and this limits its application for intracellular delivery.[4,5] EGTA-based chelators feature high Ca^{2+}/Mg^{2+} selectivity ($\sim 10^5$),[6] and their efficiency has been remarkably improved over the last 20 years[7−10] to finally obtain a NDBF-EGTA cage with excellent performance.[7] These EGTA-based chelators (NP-EGTA, NDBF-EGTA) allow fast Ca^{2+} release (see Table S1 in Supporting Information, SI, for kinetic data), which makes them currently the best choice in most experiments in neurobiology research.[1] However, the inherent sensitivity of the EGTA binding moiety to pH changes in physiological range (6.5−7.5) may result in a slower or incomplete recovery to resting Ca^{2+} after illumination since the acidification caused by uncaging changes the affinity of the cage for calcium. This fact limits the applicability of these compounds in some cases.

Photolabile BAPTA-based chelators (nitr-x) do not show pH-sensitivity in the physiological range, have high Ca^{2+}/Mg^{2+} selectivity ($\sim 10^5$), but they release Ca^{2+} rather inefficiently.[11−13] The light-induced affinity changes of nitr-x compounds is enhanced by the electron withdrawing properties of the substituents on the aromatic ring of the photoproduct. Reported nitr-x variants include one photosensitive group attached to one of the two BAPTA rings, though the possible benefit of including a second photosensitive substituent for improving the effectiveness of Ca^{2+} release has been indicated.[14] Following the double substitution concept, we describe the efficient synthesis and improved properties of BAPTA-based cages containing two photosensitive o-nitrobenzhydryl groups (nitr-T, Scheme 1) and evaluates their Ca^{2+} release in living cells. We demonstrate a general strategy to improve light-triggered Ca^{2+} release in BAPTA-chelators without compromising other properties. This strategy may open a door to preparation of more efficient, selective, pH-insensitive, and photolabile Ca^{2+} chelators.

RESULTS AND DISCUSSION

Synthesis. The chemical structure of nitr-T is shown in Scheme 1. Two o-nitrobenzhydryl groups were attached to the *p*-positions of BAPTA. For comparison the single substituted derivative (nitr-S) was also prepared. The nitr-T or −S tetraethyl esters were obtained by trimethylsilyl trifluoromethanesulfonate assisted coupling of BAPTA tetraethyl ester to 5-methoxy-2-nitrobenzaldehyde followed by treatment with tetrabutylammonium floride trihydrate (Scheme 1).[12] The intermediate esters were stable in solid state (no photolysis

Received: December 9, 2011
Published: April 22, 2012

dx.doi.org/10.1021/ja2115184 | J. Am. Chem. Soc. 2012, 134, 7733−7740

Scheme 1. Synthesis of Nitr-T and Nitr-S

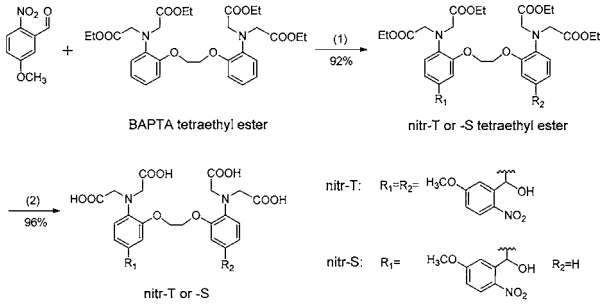

(1) i. TMS OTf, 1,6-di-ter-butylpyridine, CH_2Cl_2; ii. tetrabutylammonium floride trihydrate, $CHCl_3$; (2) NaOH, methanol/1,4-dioxane/water

after storage at room temperature for 14 days), but they photolyzed after a few hours when they were stored in solution under laboratory conditions (a $CDCl_3$ solution at room temperature showed 25% photolysis after 4 h). For this reason, immediate purification after reaction is necessary in order to obtain high yields after isolation. Hydrolysis of the ethyl esters in aqueous NaOH gave nitr-T and nitr-S. By using this synthetic route only two steps are required to obtain the nitr-T/S derivatives in good yields (total yield is 88% for nitr-T and 48% for nitr-S) and in a high purity of the crude products (e.g., nitr-T: >95%). In comparison, the reported nitr-5 required six synthesis steps with a total yield about 12%,[12] while NP-EGTA required 10 steps and the total yield was 24%.[8] Our synthesis of nitr-T/S derivatives was much simpler and efficient.

Photochemical Properties. Figure 1 presents the UV−vis spectra of nitr-T under different conditions. The absorbance

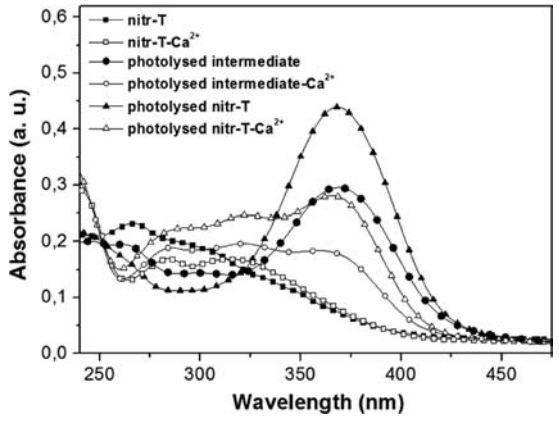

Figure 1. UV−vis spectra of a 9 μM solutions (40 mM Hepes/100 mM KCI, pH 7.2) of nitr-T, nitr-T with 240 mM $CaCl_2$, isolated photolyzed intermediate of nitr-T, photolyzed intermediate of nitr-T with 240 mM $CaCl_2$, isolated final photolyzed nitr-T photolyzed and final photolyzed nitr-T with 240 mM $CaCl_2$. See Scheme 2 for the chemical structures.

coefficients of nitr-T at 267, 350, and 360 nm in Ca^{2+}-free buffer (40 mM Hepes/100 mM KCI, pH 7.2) were 2.75×10^4, 8.23×10^3, and 6.15×10^3 $M^{-1}cm^{-1}$, respectively. Upon addition of Ca^{2+} (excess), the Ca^{2+} complex was formed and this was reflected by a significant decrease of the absorbance at 267 nm and an increase at 350 nm. Nitr-S presented a similar spectrum (see Figure S1 of the SI). The extinction coefficients of nitr-S were 4.51×10^3 and 3.4×10^3 $M^{-1}cm^{-1}$ at 350 and 360 nm, respectively, which represent nearly half the values of nitr-T at the same wavelengths. This agrees with the fact that nitr-S molecule contains a single o-nitrobenzhydryl group.

The photolysis reaction of nitr-T changed the UV spectrum and a new maximum at 380 nm appeared (Figure 1), in agreement with reported UV spectra of photolyzed nitr-5.[12] The new peak was attributed to the formation of 4-amino-2′-nitrosobenzophenone photoproducts (Scheme 2).[12] It is

Scheme 2. Photolytic Reactions of Nitr-T and Its Calcium Complex Illustrating the Photolysis Intermediates

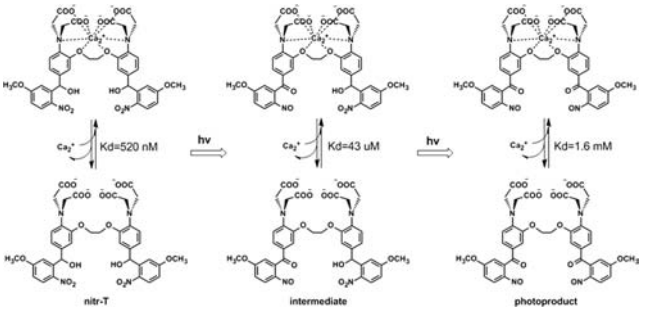

important to note that the photocleavage of nitr-T involves first the formation of a nonsymmetric (mononitrosobenzophenone)−(mononitrobenzhydryl) intermediate, which further photolyses to give the final photoproduct. To confirm this mechanism, the intermediate and final product were isolated from photolyzed mixtures and validated (see Experimental Section and Figures S10 and S11 of the SI). Therefore, three different species are present during exposure (Scheme 2). When the photolysis was performed in the presence of Ca^{2+}, a weaker maximum at 380 nm was detected which was attributed to the electron-withdrawing effect of the coordinated Ca^{2+} on the amine group of the chromophore.[15]

The photolytic conversion of nitr-T in the absence and presence of Ca^{2+} with increasing exposure was followed by UV−vis spectroscopy (Figures S2 and S3 of the SI and Figure 2a) and the composition of the photolyzed mixture for the different conversions was monitored by ^1H NMR spectroscopy (Figure S4 of the SI). The photolysis of nitr-T was quantified by the disappearance of the methylidyne proton (a) at 6.28 ppm. The ethylene protons (b) shift from 4.19 ppm (b1) in

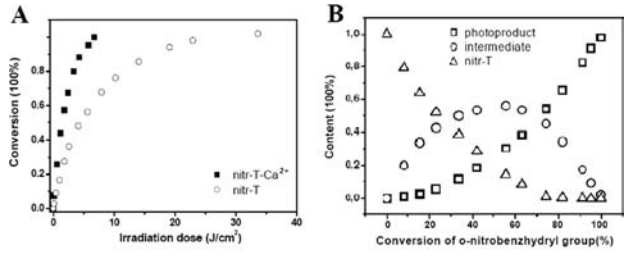

Figure 2. (A) Photolysis conversion (100%) versus irradiation doses of nitr-T and nitr-T-Ca^{2+} complex (9 μM of nitr-T and 18 μM of nitr-T-Ca^{2+} complex in 40 mM Hepes/100 mM KCI with pH 7.2). Ten mM Ca^{2+} was added for nitr-T-Ca complex and a monochromatic light of 360 nm (2.77×10^{-9} E/s) was used. (B) Composition of a nitr-T solution during photolysis. The amount of the reagent and the photoproducts was determined from the relative height of the ethylene ^1H NMR signals at 4.19, 4.24, and 4.28 ppm (b1, b2, and b3 in Figure S4 of the SI). The conversion was calculated from the integral of the proton signals at 7.04 and 7.28 (c1 and c2 in Figure S4 of the SI).

dx.doi.org/10.1021/ja2115184 | J. Am. Chem. Soc. 2012, 134, 7733−7740

nitr-T to 4.24 ppm (b2) in the intermediate product and to 4.28 ppm (b3) in the final photoproduct. The aromatic proton (c) shifted from 7.06 ppm (c1) to 7.27 ppm (c2) upon irradiation and this was attributed to the appearance of the conjugated structure. Since no other signals were observed in the NMR spectra, it was assumed that nitr-T converted to the final photoproduct nearly quantitatively. In fact, a chemical yield for the photoreaction of 94% was determined by HPLC. The composition of the photolyzed mixture at a given conversion was calculated from the ^{1}H NMR signals integrals (Figure 2). During the exposure, the concentration of nitr-T decreased while the concentration of the final photoproduct increased, and the concentration of the photolysis intermediate increased first and decreased after about 50% conversion.

The quantum yield of the photolytic reaction was calculated by ferrioxalate actinometry. A quantum yield (Φ_{360}) of 0.056 was obtained for the nitrobenzhydryl group in nitr-T. In the presence of Ca^{2+} ions, the determined Φ_{360} value was doubled (0.12). Nitr-S and nitr-S-Ca^{2+} complex showed a similar tendency of their quantum yields (0.06 for nitr-S and 0.11 for its calcium complex). It is important to note that these values are considerably higher than the reported Φ_{360} data of nitr-5 and nitr-7 (0.012 and 0.011, respectively).[1] We attribute this difference to the different methods used for quantum yield determination and the inherent error in quantum yield measurements.[16] The Ca^{2+}-induced improvement in quantum yield was also observed in nitr-5,[12] but not in EGTA-based chelators (Φ_{350} of NP-EGTA and NP-EGTA-Ca^{2+} complex were 0.23 and 0.20, respectively).[8] The photolysis reaction of nitrobenzyl compounds involves the formation of a key *aci*-nitro intermediate.[17,18] In the case of nitr-x, the resonance delocalization of electrons from para-aniline is expected to decrease the *aci*-nitro character of the intermediate, reducing the uncaging.[19] The complex with Ca^{2+} ion weakens the electron donation effect and thus, the presence of Ca^{2+} enhances the photolysis.

Ca^{2+} Binding and Release. The affinity of nitr-T for Ca^{2+} ions was obtained by titrating nitr-T solutions with incremental additions of Ca^{2+} using spectral[10] and calorimetry techniques. The concentration of the free Ca^{2+} ions $[Ca^{2+}]_F$ after the treatment of 1.0 mM solutions of nitr-T or nitr-S with various amounts of $CaCl_2$ was measured using the fluorescent dye fluo-3[20] (see Experimental Section for details). In the absence of calcium ions, the flu-3 has no fluorescence upon monochromatic (λ_{irr} = 490 nm) illumination. The addition of $CaCl_2$ triggers the emission of fluo-3 (λ_{irr} = 490 nm, λ_{em} = 530 nm) and the fluorescence intensity is proportional to the calcium ion concentration. Figure 3 shows the Ca^{2+} ion indicator fluorescence of the fluo-3 added to the nitr-T-Ca^{2+} complex solutions. From these data a value of K_d = 520 nM was obtained (see Experimental Section and ref 10 for details). This value is higher than the reported K_d of BAPTA (110 nM) or nitr-5 (145 nM) determined by spectroscopic methods.[1] The lower affinity can be attributed to the weak electron-attracting effect of the o-nitrobenzhydryl groups.

The affinity of the nitr-T photoproduct for Ca^{2+} was estimated using UV–vis spectroscopy. Figure 4 presents the titration curves of photolyzed nitr-T with $CaCl_2$. Data analysis gave a K_d of 1.6 mM for the photoproduct. It is important to note that K_d of the photoproducts of nitr-5 (6.3 μM) and nitr-7 (3.0 μM) are significantly lower as determined by same method.[12] A low binding affinity of the photoproduct is a highly desired property of phototriggerable Ca^{2+} cages, since it allows

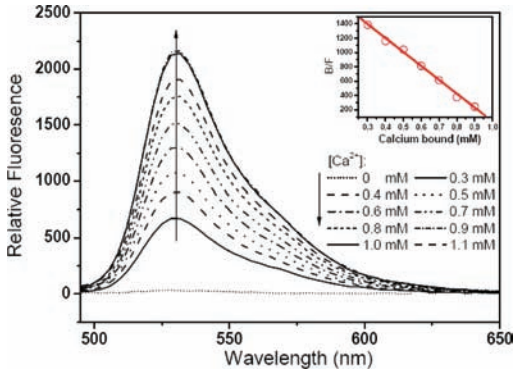

Figure 3. Emission spectra of fluo-3 (10 μM, excitation at 490 nm) resulting from titration at 20 °C of nitr-T (1.0 mM in 40 mM Hepes/100 mM KCl, pH 7.2) with 0.10 mM incremental additions of $CaCl_2$. Inset: Scatchard analysis (using a K_d value of 500 nM for fluo-3)[21] of these data.

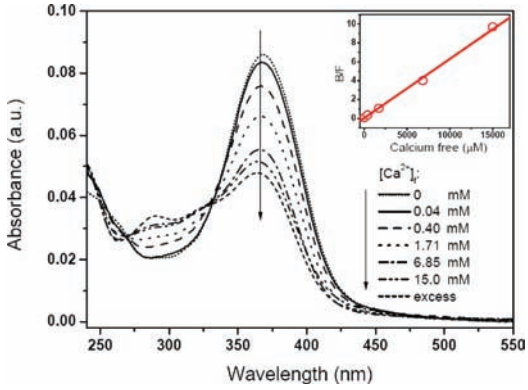

Figure 4. UV–vis spectra of photolyzed nitr-T (20 μM in 40 mM Hepes/100 mM KCl, pH 7.2) after titration with incremental additions of $CaCl_2$. Inset: Scatchard analysis of these data representing the ratio between bound (B) and free (F) concentrations of the photolyzed chelator nitr-T vs the concentration of free Ca^{2+}. $B/F = [\text{nitr-T}]_b/[\text{nitr-T}]_f = (A_{max} - A)/(A - A_{min})$, A = Absorbance at 360 nm.

higher concentrations of free Ca^{2+} after exposure.[1] The photolyzed intermediate presents an affinity of 43 μM (Figure S5 of the SI).

We measured the evolution of the free Ca^{2+} concentration in irradiated nitr-T solutions using a calcium selective electrode. Figure 5 presents these data as well as the calculated $[Ca^{2+}]_F$ for DM-nitrophen, NP-EGTA, nitr-5 and nitr-S. The concentration of the free calcium ions jumped to a very high level at about 10% conversion in the case of the DM-nitrophen. NP-EGTA also caused fairly large $[Ca^{2+}]_F$ jumps at conversions up to about 30%. In contrast, the changes in $[Ca^{2+}]_F$ in the cases of nitr-5 and nitr-S were small and continuous for all of the conversion range. Compared to this, nitr-T provided small changes at conversions lower than 50%, but it has shown strong constant response for longer photolysis. The final calcium ion concentration at full conversion almost reached the level of the NP-EGTA or DM-nitrophen.

As a consequence of the higher K_d of the chelator and lower K_d of its photodegradation product, the affinity change of nitr-T for Ca^{2+} ions upon photolysis (>3000-fold) is much higher than the affinity change of nitr-5 (43-fold) or nitr-7 (54-fold).[12] The double substitution greatly improved the Ca^{2+}-release and the final concentration of free Ca^{2+} increased up to a level

dx.doi.org/10.1021/ja2115184 | J. Am. Chem. Soc. 2012, 134, 7733–7740

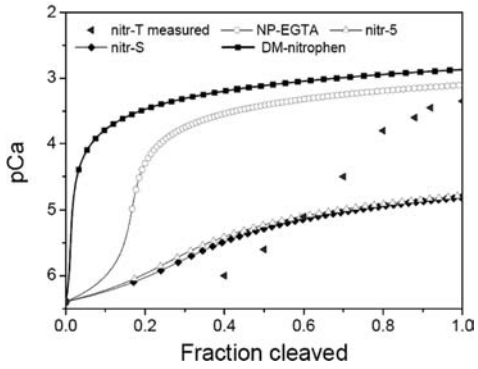

Figure 5. Changes in calcium ion concentration (pCa: $-\log[Ca^{2+}]_F$) versus photolysis conversion experimentally determined using a Ca^{2+}-electrode for nitr-T (triangles) and calculated (continuous lines) for four different calcium cages (2 mM). The initial Ca^{2+} concentration was 400 nM in all cases. $[Ca^{2+}]_T$ values: 1.975 mM for DM-nitrophen, 1.667 mM for NP-EGTA, 1.468 mM for nitr-5, 1.404 mM for nitr-S, and 0.870 mM for nitr-T.

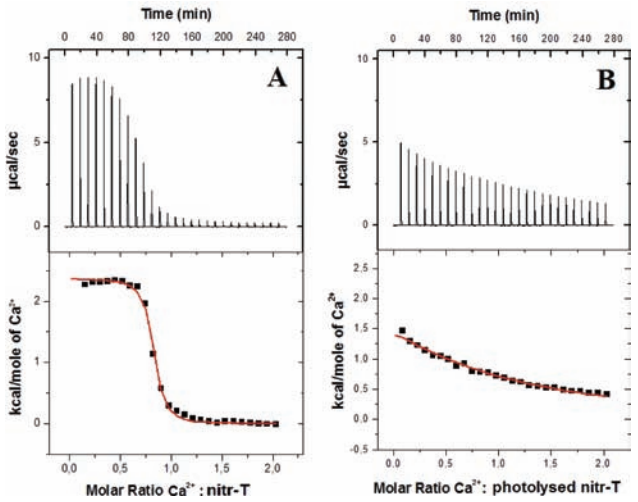

Figure 6. The microcalorimetric titrations of nitr-T (A) and of its photolytic product (B) in 40 mM HEPES (pH 7.2) containing 100 mM KCl. The raw data for the sequential injections of the 10 mM $CaCl_2$ into the 1 mM chelator are shown in the upper graphs, while the integrated heats of complexation (black squares) and the fitting to the correlation function (red lines) are depicted in the bottom panels.

comparable with EGTA-based cages. It is important to note that a 1600-fold affinity change has been indicated for a doubly substituted nitr- derivative in a review article,[14] but it was never validated by a scientific report. The K_d of nitr-S (170 nM) and of its photoproduct (6.9 μM) were estimated using the same methods (Figures S6 and S7 of the SI). An affinity change of about 40-fold upon photolysis was obtained. These values are close to those reported for nitr-5.[12]

Using the same titration method, the affinity of nitr-T for Mg^{2+} ions (28 mM, Figure S8 of the SI) was determined. The selectivity of nitr-T for Ca^{2+} against Mg^{2+} was 5×10^4 (Table S1). The value is comparable to that of nitr-5 (6×10^4)[12] and slightly smaller than NP-EGTA (11×10^4).[1]

ITC Measurement. ITC was used to determine the main thermodynamic parameters (enthalpy, entropy, affinity, stoichiometry) of the bimolecular interaction in a single experiment by measuring the heat change during the binding event.[22,23] Samples of nitr-T, nitr-S, and their photolysis products were titrated with $CaCl_2$ in buffered solutions (pH 7.2) at 25 °C. For comparison, EGTA and BAPTA were also tested. A typical graphical representation of the titration is shown in Figure 6A. Each addition of small portions of Ca^{2+} ions to the 1 mM solution of the BAPTA derivative gave an endothermic thermal response, caused by the formation of the complex between the chelator and the calcium ions. The exchanged heat decreased after each injection because less and less chelator molecules are available for complex formation. At the end of the experiment, when the calcium ions are in high excess and therefore most of the BAPTA is complexed, only the $CaCl_2$ dilution heat was detected.

The correlation of the raw data to a bimolecular interaction fitting function indicated that the positive enthalpy of the complex formation was compensated by a much higher entropic contribution. This was a common feature for all of the tested BAPTA derivatives (Table 1). In contrast, the Ca^{2+}-binding of EGTA induced a small positive entropic change and a great enthalpy decrease, suggesting an enthalpy-driving coordination.

The presence of the electron withdrawing groups on the aromatic rings caused a slight decrease of the Ca^{2+} ion affinity of the BAPTA moiety (0.86 μM for BAPTA, 3.5 μM for nitr-T, and 1.2 μM for nitr-S). The raw titration curves of the photolytic products of nitr-T and nitr-S were similar to those of nitr-T/S (Figure 6B). However, the detected affinities were significantly lower (1.5 mM for the photolyzed nitr-T and 32.6 μM for the photolyzed nitr-S) than those of the parent chelators. The calculated Ca^{2+} affinity loss of the nitr-T/S derivatives upon light exposure was 428 fold for nitr-T and 27 fold for nitr-S (Table 1). The differences in the absolute values of K_d obtained from the spectrometric and calorimetric methods are attributed to the different experimental conditions required for the experiments (i.e., different concentrations of the nitr-T/S and of the $CaCl_2$ in the tested solutions). In spite of these differences, the observed trend in both cases confirmed the significant benefit of the double substitution for light-triggered Ca^{2+}-release. The location of the strong electron-withdrawing o-nitroso-benzoyl group in the para-position to the amino-diacetate group decreased the electron density of the nitrogen atom and consequently, dramatically influenced the calcium binding properties of the molecule.

Ca^{2+} Release in Living Cells. The ability of nitr-T to release Ca^{2+} in living cells was tested in patch clamp experiments carried out in mouse chromaffin cells in primary culture. We initially examined the resting Ca^{2+} levels at different loading levels of intracellular Ca^{2+}. Cells were patch clamped in the whole cell recording mode. After a two minute equilibration period, the cell was stimulated with a UV flash generated by a flash lamp (Rapp Optoelectronics, Hamburg, Germany). Immediately after the flash application, the cell was illuminated with short (20 ms) illuminations at 350 and 380 nm at a rate of 4 Hz. This maintained the intracellular Ca^{2+} level near that reached by the flash and allowed simultaneous ratiometric Ca^{2+} measurement. Figure 7A shows the basal free Ca^{2+} (filled circles) and the free Ca^{2+} levels reached immediately after flash photolysis (determined from the ratio of the first 350/380 nm paired illumination, open circles) for a series of four different Ca^{2+} loads in the patch solution. We did not increase the Ca^{2+} load above 4 mM because we wanted to keep the resting intracellular Ca^{2+} below about 1.5 μM. The cells tolerated the loading with Nitr-T quite well. Recordings of 40 to 60 min were common with little degradation of the cell properties, which is

dx.doi.org/10.1021/ja2115184 | J. Am. Chem. Soc. 2012, 134, 7733–7740

Table 1. Calcium Binding Parameters of the nitr-T/S Chelators and Their Photolytic Products As Determined by Means of ITC and Spectroscopy

species	N^a	ΔH kcal/mol	ΔS cal/mol·K	$-T\Delta S$ kcal/mol	ΔG kcal/mol	K_d mol·l^{-1}	$K_d{}^b$ mol·l^{-1}
EGTA	0.8	−6.94 (±0.03)	5.90	−1.61	−8.550 (±0.03)	417×10^{-9} ($\pm 32 \times 10^{-9}$)	150×10^{-9}
BAPTA	1.1	2.32 (±0.01)	35.5	−9.69	−7.67 (±0.03)	0.86×10^{-6} ($\pm 0.11 \times 10^{-6}$)	110×10^{-9}
nitr-T	0.8	2.36 (±0.02)	32.9	−8.98	−6.62 (±0.03)	3.5×10^{-6} ($\pm 0.4 \times 10^{-6}$)	520×10^{-9}
photolyzed nitr-T	1.0	4.05 (±0.14)	24.5	−7.24	−3.19 (±0.14)	1.5×10^{-3} ($\pm 0.2 \times 10^{-3}$)	1.6×10^{-3}
nitr-S	0.8	2.10 (±0.02)	34.2	−9.34	−7.24 (±0.02)	1.2×10^{-6} ($\pm 0.2 \times 10^{-6}$)	170×10^{-9}
photolyzed nitr-S	0.5	2.64 (±0.15)	29.4	−8.76	−6.12 (±0.15)	32.6×10^{-6} ($\pm 3.4 \times 10^{-6}$)	6.9×10^{-6}

^{a}Stoichiometry of the $CaCl_2$:chelator complex ^{b}The corresponding values for EGTA and BAPTA are reported in ref 7; the data for nitr-T, nitr-S and for their photolytic products have been obtained by us from the spectroscopy-based determinations.

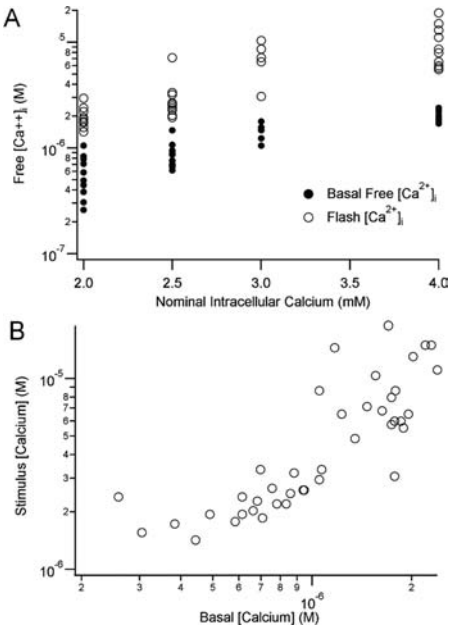

Figure 7. (A) The relationship between Ca^{2+} loading and free Ca^{2+} in nitr-T loaded cells. Chromaffin cells were patch clamped using an intracellular solution containing 6.25 mM nitr-T. This solution was complemented with added Ca^{2+} stock to reach nominal Ca^{2+} concentrations of 2 to 4 mM. The free $[Ca^{2+}]_i$ after equilibration (solid circles) the free $[Ca^{2+}]_i$ reached after flash photolysis under our normal experimental conditions (open circles) are plotted versus the nominal intracellular Ca^{2+}. The free Ca^{2+} in both cases is dependent on the loading of nitr-T. (B) Ca^{2+} concentrations reached after photolysis are dependent on the resting free Ca^{2+}. The dependence on the $[Ca^{2+}]_i$ reached after flash photolysis on the preflash $[Ca^{2+}]_i$ is shown for cells recorded after loading as described in the text.

much longer than the duration of our typical flash experiment. The amount of Ca^{2+} release was dependent on the degree of Ca^{2+} loading of nitr-T. Figure 7B is a scatter plot which shows the relationship between the basal free $[Ca^{2+}]_i$ and the response to the UV flash illumination. Under our conditions, we do not reach the upper ranges of photolytic release capacity due to relatively low loading of the nitr-T with Ca^{2+}. In spite of this low loading, we see increases of Ca^{2+} to low μM concentrations with 2 mM Ca^{2+} added to 6.25 mM nitr-T. At 3−4 mM added Ca^{2+}, calcium release can approach 10 to 20 μM, depending on the conditions. Thus, these experiments show the successful release of Ca^{2+} from nitr-T in living cells. Higher Ca^{2+} loading would result in unacceptably high $[Ca^{2+}]_i$. However, at lower added Ca^{2+} (~35% saturation) we were still able to generate appreciable increases in $[Ca^{2+}]_i$. The resting free $[Ca^{2+}]$ in chromaffin cells is near 100 nM. Priming is calcium sensitive and at resting Ca^{2+} the releasable pools are quite small. For this reason, we generally load NP-EGTA to generate free calcium in the range of 500−700 nM, which leads to increased photolysis induced catecholamine release. Typically, loading to about 80% of added NP-EGTA (e.g., 4 mM Ca^{2+} and 5 mM NP-EGTA) produces cytosolic free Ca^{2+} near 350 nM. Using nitr-T, we reached acceptable resting free Ca^{2+} levels with up to 2.5 mM Ca^{2+} added to 6.5 mM nitr-T, (free Ca^{2+} typically near 700−800 nM). In experiments requiring a resting (prephotolysis) calcium concentration closer to the physiological resting level in most cells (50−250 nM), less calcium may be added, and therefore less nitr-T will be loaded with Ca^{2+}, due to its relatively low prephotolysis Ca^{2+} affinity. Under these conditions, photolysis of nitr-T will result in smaller increases in free Ca^{2+}, limiting its efficacy.

Ca^{2+} released by flash photolysis effectively elicited vesicle fusion in chromaffin cells loaded with nitr-T (Figure 8A).

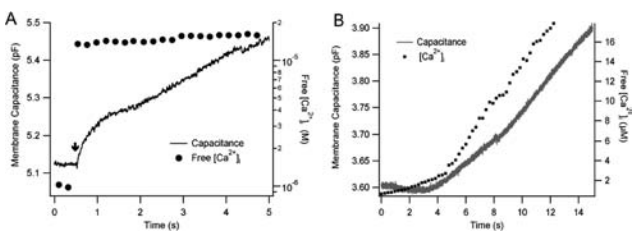

Figure 8. (A) Membrane capacitance, recorded by patch clamp in the whole cell configuration (solid line) following flash photolysis of nitr-T. The free $[Ca^{2+}]_i$ (solid circles) is shown prior to and after flash photolysis. (B) Monochromator elicited Ca^{2+} ramp stimulation also drives membrane fusion by photolysis of nitr-T. In patch clamped chromaffin cells loaded with nitr-T as described above, application of trains of alternating illumination at 350 and 380 nm (20 ms duration) at 4 Hz slowly raised free $[Ca^{2+}]_i$ (squares) and caused fusion of vesicles, resulting in a capacitance increase (solid line).

Exocytosis of large dense cored vesicles, as tracked by membrane capacitance changes, demonstrated that photolyzed Ca^{2+} is available to elicit Ca^{2+} dependent cellular processes. Membrane capacitance, recorded by patch clamp in the whole cell configuration rose significantly following flash photolysis of nitr-T.

We have also applied trains of alternating 350 and 380 nm illuminations utilizing the monochromator, to slowly photolytically release Ca^{2+} without flash application (ramp stimulation) from nitr-T (with simultaneous monitoring of free Ca^{2+}) and found that this method also generates effective Ca^{2+} release which also drove vesicle fusion with the plasma membrane. Figure 8B shows one such experiment in which a chromaffin cell with a baseline Ca^{2+} near 400 nM was

dx.doi.org/10.1021/ja2115184 | J. Am. Chem. Soc. 2012, 134, 7733−7740

illuminated at 4 Hz for 12 s. The intracellular Ca^{2+} (filled squares) rose during the train of illuminations and as it approached 1 μM the membrane capacitance (solid line) began to rise, indicating fusion of vesicles with the plasma membrane. Thus nitr-T can also release Ca^{2+} under more moderate UV illumination.

CONCLUSIONS

The properties of doubly functionalized nitr-T reported in this manuscript demonstrate that nitr-T is a potential new Ca^{2+} ion cage for cell biology with greatly improved release efficiency against the singly substituted nitr-x chelators, while maintaining their pH insensitivity in the physiological range and the high Ca^{2+}/Mg^{2+} selectivity. Our patch clamp experiments show that nitr-T is well tolerated by the living cells. Moderate Ca^{2+} jumps were generated using exposure conditions compatible with sub μM resting $[Ca^{2+}]$. At low amounts of the added Ca^{2+} (~35% loading), we were able to generate appreciable increases in $[Ca^{2+}]_i$. Under conditions where higher resting $[Ca^{2+}]_i$ can be tolerated, larger Ca^{2+} jumps could be generated. Further improvement of the releasing and photolytic properties of the doubly functonalized nitr-T by using other chromophores attached to the BAPTA ring can be envisioned and are currently in progress in our group.

EXPERIMENTAL SECTION

Materials and Methods. 5-Hydroxy-2-nitro-benzaldehyde (97%, Sigma-Aldrich), iodomethane (99%, Sigma-Aldrich), trimethylsilyl trifluoromethanesulfonate (TMS OTf, 98%, Sigma-Aldrich), 2,6-di-*tert*-butylpyridine (97%, Sigma-Aldrich), BAPTA tetraethyl ester (98%, Alfa), KCl (99%, $Ca^{2+}{}_{max}$ < 0.001%, Riedel-de Haën), and solvents were used as purchased. Preparative column chromatography and flash column chromatography were carried out using silica gel (60 Å pore size, 63−200 μm particle size) from MerckK GaA (Darmstadt,Germany).

Solution ^1H and ^{13}C spectra were measured in $CDCl_3$ or DMSO-d_6 solution at 25 °C with a Bruker Ultra Shield 250 MHz spectrometer. UV spectra were recorded on a Varian Cary 4000 UV−vis spectrometer (Varian Inc. Palo Alto, CA). Fluorescence spectra were obtained from TIDA S400 fluorescence spectrometer (J&M, Germany). Mass spectra were recorded on a Micromass Finnigan-MAT ZAB-HS mass spectrometer. A calcium ion-selective electrode (Orion type 9720BNWP, Pulse Instruments, U.S.) was used for determining the free Ca^{2+} concentrations. HPLC analysis and purification of the compounds were performed with a JASCO HPLC 2000 (Jasco, Groß-Umstadt, Germany) equipped with a diode array UV−vis detector and fraction collector. Reprosil 100 C18 columns were used for preparative (250 × 20 mm) and analytical (250 × 5 mm). Water containing 0.1% TFA and acetonitrile containing 5% water and 0.1% TFA were used as eluents. Analytical and preparative runs were performed at a solvent flow of 1 mL/min and 10 mL/min, respectively, and by increasing the volume fraction of acetonitrile after a 3 min run from 0% to 100% within 30 min and successively keeping this ratio for another 7 min.

Synthesis. *5-Methoxy-2-nitrobenzaldehyde.*[24] A mixture of 5-hydroxy-2-nitro-benzaldehyde (1.0 g, 6 mmol), iodomethane (0.75 mL, 12 mmol), and potassium carbonate (4.13 g, 30 mmol) in 50 mL of DMF was stirred for 12 h at rt. The resulting yellow suspension was filtered and the solid was washed with dichloromethane. The filtrate and washing solutions were combined and dried over Na_2SO_4. The organic solvent was removed under reduced pressure and the solid was recrystallized from a mixture of ethyl acetate/petroleum ether to yield 0.73 g yellow needle crystal solid. Yield: 67%. ^1H NMR (250 MHz, $CDCl_3$, δ ppm): 10.41 (s, H, CHO), 8.10−8.06 (d, H, aromatic), 7.26−7.24 (d, H, aromatic), 7.09−7.05 (dd, H, aromatic), 3.87 (s, 3H, OCH_3).

1,2-Bis{2-amino-5-[(5-methoxy-2-nitrophenyl)hydroxymethyl]-phenoxy}ethane-N,N,N′,N′-tetraacetic Acid Tetraethyl Ester (Nitr-T Tetraethyl Ester). In a dark environment, trimethylsilyl trifluoromethanesulfonate (TMS OTf) (0.544 mL, 2.72 mmol) was added dropwise into a solution of BAPTA tetraethyl ester (160 mg, 0.272 mmol), 5-methoxy-2-nitrobenzaldehyde (130 mg, 0.72 mmol), and 2,6-di-*tert*-butylpyridine (0.72 mL, 3.26 mmol) in dry CH_2Cl_2 (4 mL) at room temperature under inert atmosphere. TLC and ^1H NMR suggested the reaction finished after stirring in dark environment for 72 h. The reaction solution was diluted with CH_2Cl_2 (10 mL), poured into saturated aqueous $NaHCO_3$ (50 mL) and the organic phase was then separated. The aqueous layer was extracted with CH_2Cl_2. The combined extracts were washed with water, dried over Mg_2SO_4, and evaporated to dryness to yield a yellow oil. The oil was dissolved in $CHCl_3$ (30 mL) and tetrabutylammonium fluoride trihydrate (260 mg, 0.82 mmol) was added. After 30 min stirring in a dark environment at room temperature, the solution was evaporated to dryness, following by dissolved in ethyl acetate-toluene (1:1 v/v, 100 mL), washed with water, dried over Mg_2SO_4, and the solvent was evaporated to yield the crude product as orange oil. The crude product was purified immediately by silica flash column with ethyl acetate−hexane (1:1) as eluant (R_f: 0.4) afforded the pure product (238 mg, yellow solid, yield 92%). The product was immediately used for the next step. ^1H NMR (250 MHz, $CDCl_3$, δ ppm): 8.08−8.04 (dd, 2H, aromatic), 7.36−7.34 (t, 2H, aromatic), 6.91−6.86 (m, 4H, aromatic), 6.73−6.68 (m, 4H, aromatic), 6.46 (s, 2H, ArCH), 4.21−4.19 (d, 4H, OCH_2CH_2O), 4.10 (s, 8H, NCH_2), 4.07−3.96 (m, 8H, OCH_2), 3.91 (s, 3H, OCH_3), 1.16−1.10 (m, 12H, CH_2CH_3). ^{13}C NMR (62.5 MHz, $CDCl_3$, δ ppm): 171.53 (C═O), 163.68, 149.93, 142.19, 140.76, 139.07, 135.67, 127.90, 120.02, 118.35, 114.03, 112.88, 112.63 (12C, aromatic), 71.42 (ArCH), 67.11 (OCH_2CH_2O), 60.89 (OCH_2), 55.94 (OCH_3), 53.44 (NCH_2), 14.00 (CH_2CH_3). MS ($C_{46}H_{56}N_4O_{18}{}^{2+}$): 952.6 (Calculated 952.9).

Nitr-S Tetraethylester. An analogous method was used to synthesize the nitr-S, with the difference that the molar ratio of BAPTA tetraethyl ester: 5-methoxy-2-nitrobenzaldehyde: TMS OTf was 1:1:1. Yield: 50%. ^1H NMR (250 MHz, $CDCl_3$, δ ppm): 8.00−7.96 (d, 1H, aromatic), 7.23−7.22 (d, 1H, aromatic), 6.82−6.72 (m, 6H, aromatic), 6.69−6.60 (m, 2H, aromatic), 6.38 (s, 2H, ArCH), 4.17 (s, 4H, OCH_2CH_2O), 4.06 (s, 4H, NCH_2), 4.05(s, 4H, NCH_2), 3.99−3.91 (m, 8H, OCH_2), 3.91 (s, 3H, OCH_3), 1.08−1.03 (m, 12H, CH_2CH_3).

1,2-Bis{2-amino-5-[(5-methoxy-2-nitrophenyl)hydroxymethyl]-phenoxy}ethane-N,N,N′,N′-tetraacetic Acid (Nitr-T). Nitr-T tetraethyl ester (200 mg, 0.21 mmol) was dissolved in a mixture of methanol (10 mL) and 1,4-dioxane (5 mL) and then saponified by the addition of an excess of 1 M aqueous NaOH and stirring overnight at room temperature. After acidification with HCl aqueous to pH 3, the precipitate was collected and dried to afford the product (169 mg, yellow solid). Yield: 96%. ^1H NMR (250 MHz, DMSO-d_6, δ ppm): 8.02−7.98 (dd, 2H, aromatic), 7.40−7.39 (d, 2H, aromatic), 7.06−7.05 (d, 2H, aromatic), 6.94 (s, 2H, aromatic),6.67−6.63 (m, 4H, aromatic), 6.29 (s, 2H, ArCH), 4.21 (s, 4H, OCH_2CH_2O), 4.02 (s, 8H, NCH_2), 3.88 (s, 6H, OCH_3). ^{13}C NMR (62.5 MHz, $CDCl_3$, δ ppm): 172.80 (C═O), 162.96, 149.02, 143.10, 140.44, 138.10, 135.83, 127.22, 119.80, 117.69, 113.61, 113.49, 112.72 (12C, aromatic), 69.24 (ArCH), 67.19 (OCH_2CH_2O), 55.96 (OCH_3), 53.44 (NCH_2). MS ($C_{38}H_{38}N_4O_{18}Na^+$): 861 (Calculated 861.2). Elemental Anal. Calculated for $C_{38}H_{38}N_4O_{18}$: C, 54.42; H, 4.57; N, 6.68. Found: C, 54.19; H, 4.39; N, 6.59.

1-{2-Amino-5-[(5-methoxy-2-nitrophenyl)hydroxymethyl]-phenoxy}-2-(2-amino-phenoxy)ethane-N,N,N′,N′-tetraacetic Acid (Nitr-S). Yield: 96%. ^1H NMR (250 MHz, DMSO-d_6, δ ppm): 8.01−7.98 (d, 1H, aromatic), 7.39−7.38 (d, 1H, aromatic), 7.06−6.75 (m, 6H, aromatic), 6.65−6.61 (m, 2H, aromatic), 6.28 (s, 1H, ArCH), 4.23 (s, 4H, OCH_2CH_2O), 4.04 (s, 4H, NCH_2), 4.01(s, 4H, NCH_2), 3.88 (s, 3H, OCH_3). MS ($C_{30}H_{31}N_3O_{14}Na^+$): 680 (Calcd. 680.2). Anal. Calcd. for $C_{30}H_{31}N_3O_{14}$: C, 54.80; H, 4.75; N, 6.39. Found: C, 54.61; H, 4.59; N, 6.21.

dx.doi.org/10.1021/ja2115184 | J. Am. Chem. Soc. 2012, 134, 7733−7740

1,2-Bis{2-amino-5-[(5-methoxy-2-nitrosophenyl)carbonyl]-phenoxy}ethane-N,N,N′,N′-tetraacetic Acid (Final Photolysis Product of Nitr-T). A solution of nitr-T in DMSO (1 mL, 10 mg/mL) was irradiated under 360 nm with 180 J/cm^2 and then the photoproduct was isolated with preparative HPLC. After removed the solution by freeze-drying, 1.8 mg yellow powder was obtained. The product was used immediately. ^{1}H NMR (250 MHz, DMSO-d_6, δ ppm): 7.65−7.62 (dd, 2H, aromatic), 7.50−7.49 (d, 2H, aromatic), 7.29−7.25 (dd, 2H, aromatic), 7.19−7.18 (d, 2H, aromatic),6.97−6.93 (dd, 2H, aromatic), 6.54−6.50 (d, 2H, aromatic), 4.30 (s, 4H, OCH_2CH_2O), 4.15 (s, 8H, NCH_2), 3.99 (s, 6H, OCH_3). MS ($C_{38}H_{34}N_4O_{16}Na^+$): 825 (Calcd. 825.2). HPLC analysis suggested a purity of 97%.

1-{2-Amino-5-[(5-methoxy-2-nitrosophenyl)carbonyl]phenoxy}-2-{2-Amino-5-[(5-methoxy-2-nitrophenyl)hydroxymethyl]phenoxy}-ethane-N,N,N′,N′-tetraacetic Acid (Photolysis Intermediate). A solution of nitr-T in DMSO (2 mL, 10 mg/mL) was irradiated under 360 nm with 100 J/cm^2 and then isolated as photolyzed nitr-T. 0.6 mg yellow powder was obtained after HPLC purification. The product was used immediately. ^{1}H NMR (250 MHz, DMSO-d_6, δ ppm): 8.01−7.98 (d, 1H, aromatic), 7.68−7.63 (dd, 1H, aromatic), 7.50 (s, 1H, aromatic), 7.39−7.37 (d, 1H, aromatic), 7.30−7.25 (dd, 1H, aromatic), 7.17−7.16 (d, 1H, aromatic), 7.06−7.01 (dd, 1H, aromatic), 6.96−6.94 (m, 2H, aromatic), 6.68−6.60 (m, 2H, aromatic), 6.58−6.52 (t, 1H, aromatic), 6.29 (s, 1H, ArCH), 4.29−4.20 (t, 4H, OCH_2CH_2O), 4.16 (s, 4H, NCH_2), 4.03 (s, 4H, NCH_2), 3.99 (s, 3H, OCH_3), 3.88 (s, 3H, OCH_3). MS ($C_{38}H_{36}N_4O_{17}Na^+$): 843 (Calcd. 843.2). HPLC analysis suggested a purity of 93%.

Irradiation Conditions and Quantum Efficiency. A LUMOS 43 lamp (Atlas Photonics) equipped with a LED at 360 nm was used for the experiments. The quantum flow of the lap was 2.77×10^{-9} E/s as measured by ferrioxalate actinometry. For the evaluation of the quantum yield of the photouncaging reaction, the number of reacted molecules (i.e., the conversion) for a given exposure time (i.e., the number of photons) was determined by ^{1}H NMR and UV spectroscopy for conversions below 10%. For these experiments 2.5 mL of a 6 mM solution of either nitr-T or nitr-S in Na_2HPO_4/$NaHPO_4$ buffer (in D_2O, 0.044 wt % of $NaHPO_4$ and mol 0.18 wt % Na_2HPO_4) at pH 7.2 was used and various portions of 17 mM $CaCl_2$ were added to each aforementioned solution in the case of the nitr-T/S−Ca^{2+} complexes photolysis experiments.

Ca^{2+} Binding Affinity. The stability constant for the equilibrium binding of Ca^{2+} to the chelators nitr-T or nitr-S (K_a) was calculated using the method of Ellis-Davies et al.[10] by the equation:

$$K_a([\text{nitr} - T/S]_T - [Ca^{2+}]_B) = [Ca^{2+}]_B/[Ca^{2+}]_F$$

where $[Ca^{2+}]_F$ is the concentrations of the free Ca^{2+}, $[Ca^{2+}]_B$ is the concentration of Ca^{2+} bound to the chelator, and $[\text{nitr-T}]_T$ or $[\text{nitr-S}]_T$ the total concentration of the chelator in the solution. The values of $[Ca^{2+}]_F$ (and hence $[Ca^{2+}]_B$) were obtained by measuring the emission of a calcium-sensitive dye (fluo-3, K_d = 500 nM) during the titration with 0.10 mM $CaCl_2$.[8]

In this experiment, 1.0 mM solutions of the chelators in 40 mM Hepes pH 7.2 + 100 mM KCl have been used.

After the full light exposure, the estimates of $[Ca^{2+}]_B/[Ca^{2+}]_F$ were obtained from the absorption curves by the method described previously.[12] The concentration of nitr-T used for irradiation was 20 μM and the concentrations of $CaCl_2$ were 0.04, 0.40, 1.71, 6.85, 15.0, and 240 mM, respectively (further increase the concentration did not change the absorption curve any more). The $[Ca^{2+}]_F$ is close to $[Ca^{2+}]_T$ due to the fact that the concentration of the calcium ions is significantly higher that the chelators concentrations. The $[Ca^{2+}]_B$ (= $[\text{chelator}]_B$) was obtained from the UV−vis spectra by measuring the absorbance of the chelator solutions in the presence and in the absence of $CaCl_2$. The equation:

$$[\text{chelator}]_B/[\text{chelator}]_F = (A_{max} - A_x)/(A_x - A_{min})$$

(where A_{max} is the absorbance of the chelator without Ca^{2+}, A_{min} is the absorbance of the chelator in the presence of a high excess of Ca^{2+}, and A_x is the absorbance with setted Ca^{2+} concentration) gave the complexed chelator concentration.

This method was also used to calculate the affinity of chelator-Mg^{2+} before irradiation under similar condition. The concentration of photoproducts (photolyzed nitr-T/S) used was 10 μM. The solutions were buffered to pH 7.2 with 40 mM Hepes and the ionic strength was set with 100 mM KCl.

Experimental Determination of the Free Ca^{2+} Using the Ion-Selective Calcium Electrode. The calcium electrode was calibrated at 20 °C using a 0.1 M $CaCl_2$ calibration standard solution diluted to concentrations between 1×10^{-2} M, and 4×10^{-7} M. A sample containing 2 mM nitr-T and 0.87 mM Ca^{2+} was used for the experiments (data in Figure 5) and irradiated for various times. The concentration of the free Ca^{2+} was determined by interpolating the measured values in the calibration curve. The corresponding conversion of nitr-T for each irradiation time was calculated by ^{1}H NMR spectroscopy.

Isothermal Titration Calorimetry (ITC). Titration calorimetry measurements were performed with a VP-ITC calorimeter (Microcal, Northampton, MA). In a typical experiment, 27 aliquots of 10 μL buffered (40 mM HEPES pH 7.2 containing 100 mM KCl) solution of 3.3 mM $CaCl_2$ were added into the measuring cell containing 1.4 mL of the calcium chelator (330 μM in the same buffer) using a 250 μL rotating syringe at constant temperature (25 °C). The gap between two consecutive injections was set to 10 min, in order to allow the system to reach the thermodynamic equilibrium between injections. The heat change associated with the dilution of the $CaCl_2$ into buffer was determined (control experiments), using the same number of injections and the same $CaCl_2$ concentration as employed in the titration experiment. The heat of interaction for each injection was measured by the integration of each titration peak using the ORIGIN 7 software (OriginLab Co. Northampton, MA, delivered with the VP-ITC). For each injection, the dilution heats in the control experiment were subtracted from the heat obtained in the interaction experiment. The resulting corrected curves with the heat of the interaction were used for the calculations of the stoichiometry, molar enthalpy, equilibrium constant, entropy, and Gibbs free energy of the complexation. The thermodynamic parameters were determined by applying the correlation function corresponding to one binding site model. The experiments were performed using nitr-T, nitr-S and their photolysis products after HPLC purification.

Evaluation of Ca^{2+} Release in Living Cells. Calcium release from nitr-T in living cells was tested under quasi-physiological conditions. nitr-T was applied as a component of the intracellular solution in patch clamp experiments carried out in mouse chromaffin cells in primary culture. The nitr-T was dissolved in 20 mM HEPES/CsOH solution. The resulting 20 mM nitr-T-Hepes solution was added to Cs-glutamate to reach a final concentration of 6.25 mM nitr-T and 6.25 mM Hepes. The intracellular solution also contained 2 mM MgATP, 0.5 mM Na-GTP, 200 μM MagFura and Fura4F, and 2−4 mM $CaCl_2$. The final pH was 7.32 and the final osmolarity was 291 mOsm.

Whole cell recordings were carried out in mouse chromaffin cells. The methods for cell preparation and experimental procedures have been previously described.[25] A monochromator (Till Photonics, Planegg, Germany) was used to induce photolysis by illumination at 350 and 380 nm in ramp experiments, which allowed simultaneous ratiometric determination of the free intracellular calcium, by extrapolation to an in vivo calibration curve generated for the dye mixture.[26] In addition to monitoring changes in the ratiometrically determined intracellular free calcium, we used increases in membrane capacitance as an independent readout for the efficacy of released calcium to trigger membrane fusion of large dense core granules.

■ ASSOCIATED CONTENT

Ⓢ Supporting Information

UV spectra, fluorescence spectra, ^{1}H NMR spectra, and the table collecting the properties of calcium caged compounds. This material is available free of charge via the Internet at http://pubs.acs.org.

AUTHOR INFORMATION

Corresponding Author

delcampo@mpip-mainz.mpg.de

Notes

The authors declare no competing financial interest.

ACKNOWLEDGMENTS

A.d.C., J.C., and R.A.G. acknowledge financial support from the DFG (Projects CA880/3-1) and from the Materials World Network Program (DFG AOBJ 569628).

REFERENCES

(1) Ellis-Davies, G. C. R. *Chem. Rev.* **2008**, *108*, 1603−1613.
(2) Ellis-Davies, G. C. R. *Nat. Methods* **2007**, *4*, 619−628.
(3) Mayer, G.; Heckel, A. *Angew. Chem., Int. Ed.* **2006**, *45*, 4900−4921.
(4) Ellis-Davies, G. C. R. *Methods Enzymol.* **2003**, *360*, 226−238.
(5) Murphy, E.; Freudenrich, C. C.; Lieberman, M. *Annu. ReV. Physiol.* **1991**, *53*, 273−287.
(6) Tsien, R. Y. *Biochemistry* **1980**, *19*, 2396−2404.
(7) Momotake, A.; Lindegger, N.; Niggli, E.; Barsotti, R. J.; Ellis-Davies, G. C. R. *Nat. Methods* **2006**, *3*, 35−40.
(8) Ellis-Davies, G. C. R.; Kaplan, J. H. *Proc. Natl. Acad. Sci. U. S. A.* **1994**, *91*, 187−191.
(9) DelPrincipe, F.; Egger, M.; Ellis-Davies, G. C. R.; Niggli, E. *Cell Calcium* **1999**, *25*, 85−91.
(10) Ellis-Davies, G. C. R.; Barsotti, R. J. *Cell Calcium* **2006**, *39*, 75−83.
(11) Gurney, A. M.; Tsien, R. Y.; Lester, H. A. *Proc. Natl. Acad. Sci. U. S. A.* **1987**, *84*, 3496−3500.
(12) Adams, S. R.; Kao, J. P. Y.; Grynkiewicz, G.; Minta, A.; Tsien, R. Y. *J. Am. Chem. Soc.* **1988**, *110*, 3212−3220.
(13) Adams, S. R.; Lec-Ram, V.; Tsien, R. Y. *Chem. Biol.* **1997**, *4*, 867−878.
(14) Adams, S. R.; Tsien, R. Y. *Annu. Rev. Physiol.* **1993**, *55*, 755−784.
(15) Tsien, R. Y. *Annu. Rev. Biophys. Bioeng.* **1993**, *12*, 91−116.
(16) The difference in the quantum yields reported by Tsien and those reported here seem to originate from the different calculation method. We have obtained the quantum yield values in our manuscript by ferrioxalate (see Experimental Section). Tsien calculated the quantum yield for nitr-5 and nitr-7 using $(I\varepsilon t_{90\%})^{-1}$, where I is the irradiation intensity in einsteins cm^{-2} s^{-1}, ε is the decadic extinction coefficient in cm^2 $(mol\ substrate)^{-1}$, and $t_{90\%}$ is the irradiation time in seconds for 90% conversion to product. In our case, 90% conversion of nitr-T to the final photoproduct requires 96% conversion of the nitrobenzhydryl groups (determined by ^1H NMR, as shown in Figure 2b). Resulting values of the quantum yield for nitr-T and nitr-S applying Tsiens methods are 0.005 and 0.013, respectively. These values agree with those reported by Tsien for nitr-5 and nitr-7.
(17) Yip, R. W.; Sharma, D. K.; Giasson, R.; Gravel, D. *J. Phys. Chem.* **1984**, *88*, 5770−5772.
(18) Yip, R. W.; Sharma, D. K.; Giasson, R.; Gravel, D. *J. Phys. Chem.* **1985**, *89*, 5328−5330.
(19) Kennedy, D. P.; Brown, D. C.; Burdette, S. C. *Org. Lett.* **2010**, *12*, 4486−4489.
(20) Minta, A.; Kao, J. P. Y.; Tsien, R. Y. *J. Biol. Chem.* **1989**, *264*, 8171−8178.
(21) Harkins, A. B.; Kurebayashi, N.; Baylor, S. M. *Biophys. J.* **1993**, *65*, 865−881.
(22) Velázquez-Campoy, A.; Ohtaka, H.; Nezami, A.; Muzammil, S.; Freire, E. In *Current Protocols in Cell Biology*; John Wiley & Sons, Inc.: New York, 2001.
(23) Stevens, D.; Wu, Z.; Matti, U.; Junge, H.; Schirra, C.; Becherer, U.; Wojcik, S.; Brose, N.; Rettig, J. *Curr. Biol.* **2005**, *15*, 2243−2248.
(24) Widler, L.; Altmann, E.; Beerli, R.; Breitenstein, W.; Bouhelal, R.; Buhl, T.; Gamse, R.; Gerspacher, M.; Halleux, C.; John, M. R.; Lehmann, H.; Kalb, O.; Kneissel, M.; Missbach, M.; Müller, I. R.; Reidemeister, S.; Renaud, J.; Taillardat, A.; Tommasi, R.; Weiler, S.; Wolf, R. M.; Seuwen, K. *J. Med. Chem.* **2010**, *53*, 2250−2263.
(25) Liu, Y.; Schirra, C.; Stevens, D.; Matti, U.; Speidel, D.; Hof, D.; Bruns, D.; Brose, N.; Rettig, J. *J. Neurosci.* **2008**, *28*, 5594−5601.
(26) Thomas, V. *Neuron* **2000**, *28*, 537−545.